THE AMERICAN SOCIETY OF MECHANICAL ENGINEERS
345 E. 47th St., New York, N.Y. 10017

96-GT-62

COMPRESSOR OFF-DESIGN PERFORMANCE PREDICTION USING AN ENDWALL MODEL

John Dunham

BREAK

Propulsion Technology Department
Defence Research Agency
Pyestock, Farnborough, Hampshire, GU14 0LS
United Kingdom

ABSTRACT

A throughflow method for designing and analysing compressors has to be supplied with loss, deviation, and blockage estimates for every blade row. The earliest methods used empirical correlations for profile loss and deviation, together with an empirical blockage or "work done" factor, and empirical estimates of additional losses near the endwalls. Previous papers by the author have described how to replace the empirical blockage factor and endwall corrections by explicit calculations using a new mathematical model of the endwall phenomena. Those papers illustrated the application of the method near design conditions, using either design profile loss and deviation figures or computations by a viscous-inviscid interaction blade-to-blade method.

In order to estimate off-design performance rapidly over the whole operating range, some way of estimating off-design profile loss and deviation must be chosen. In this paper, the previously-derived design point loss and deviation figures are retained, and an empirical correlation due to Miller, Wasdell, and Wright is used to predict the changes in loss and deviation off-design. It is shown by means of sample three-dimensional Navier-Stokes computations that the endwall model remains applicable off-design.

The method has been tested against two low speed and two high speed compressors, one of each example having controlled-diffusion blading. The low speed compressor characteristic maps are predicted only approximately, but the predicted high speed compressor maps are good. It is widely believed that endwall flow separation can initiate stall or surge. As stall or surge was approached the shape factor of the annulus wall boundary layer at one location rose sharply, but no single stall-predicting value could be found.

NOMENCLATURE

H	shape factor
i	incidence
M_1	inlet Mach number
o/s	throat/pitch
s/c	pitch/chord
α	inlet gas angle
β_1	inlet metal angle
δ	deviation
ϕ	flow coefficient=axial velocity/blade speed
γ	ratio of specific heats
θ	camber
ω	pressure loss coefficient
ξ	stagger

Subscripts

c	choking
ml	minimum loss
neg	negative incidence stall
opt	optimum incidence
s	stall

1. INTRODUCTION

An aeroengine compressor is required to operate over a wide range of conditions, not just at its nominal design point. The highest efficiency is needed at cruise, although take-off may be the nominal design point. When designing the blading, it is essential to check that the surge and choke margins will be adequate at all speeds, and it is helpful to know the incidence and Mach number range over which individual blade sections will operate. An estimate of the overall characteristics of the

Presented at the International Gas Turbine and Aeroengine Congress & Exhibition
Birmingham, UK — June 10-13, 1996

compressor over its complete operating range is obviously desirable.

Many current design procedures use the S1/S2 approach (Calvert and Ginder, 1985, for example), at least initially. This involves the use of a throughflow code (S2) linked to a blade-to-blade code (S1) run at several spanwise stations on every blade row. It has proved very effective at or near "design" conditions, which are characterised by local incidence angles around optimum incidence at all these spanwise stations. It has also been used at near-surge conditions at design speed. But the S1/S2 approach has not generally been used to estimate the full range of overall performance characteristics for two reasons:

(1) an S1 computation takes some time to complete, even on a fast computer, and at very high or very low incidences it may not converge, so the S1/S2 computation of the complete characteristic may well take several days.

(2) there is as yet no reliable way of predicting surge in the S1/S2 scheme.

A possible alternative might be to use one of the steady-flow three-dimensional Navier-Stokes codes now available to manufacturers. They are widely used for designing single blade rows or stages (especially civil fan blades). But only recently has there been any evidence that they are capable of predicting the performance of a multistage unit; and their computation times and costs are even higher. So recourse is often made to the simplest method, the one-dimensional stage-stacking approach (Howell and Calvert, 1978, for example), which, suitably calibrated against similar design styles, can give a good estimate of overall characteristics, including an idea of the surge line.

The purpose of the present paper is to explore the extent to which throughflow (S2) methods could improve on these approaches, by estimating not only overall performance but the operating range of every aerofoil section, and possibly even giving an indication of where and when surge may be initiated.

When throughflow methods were first developed in the 1960s, no S1 computation was available, and empirical correlations of cascade measurements were used to provide estimates of deviation and loss coefficients. These correlations covered the whole range of incidence and could be built into the S2 codes. However, the correlations covered only the families of standard profile shapes used in those days; modern tailored profiles have lower losses and deviation. So it would be no good simply reverting to them for a modern design.

The empirical correlations are often based on the following approach. First, the incidence for minimum loss is estimated. At that "reference" condition, the deviation and nominal loss are evaluated. Changes in loss and deviation at other conditions are then correlated as functions of the change in incidence. This paper describes a new hybrid scheme, employing the results of the S1/S2 computation at the design point to generate the "reference" deviation and loss values (instead of using an outdated correlation) but then reverting to a correlation to estimate the *changes* in loss and deviation at off-design conditions.

The problem of surge line prediction remains. There has long been a view amongst some compressor analysts that what triggers surge is not usually aerofoil stall but endwall stall, leading rapidly to a massive flow separation either at the hub or the casing (depending on the design of the blading). Since the S2 scheme employed here explicitly calculates the annulus wall boundary layers (AWBLs), it is tempting to see if the AWBL shape factor (the criterion for separation of a conventional boundary layer) is an indicator of impending surge.

Two very different test cases have been selected to judge the extent to which this approach works:

(1) Two versions of the four-stage low speed research compressor tested at Cranfield by Robinson (1991), and

(2) The four-stage and five-stage versions of the C147 high speed core compressor tested at Pyestock (Calvert *et al*, 1989, and Ginder, 1991).

In earlier papers (Dunham, 1993 and 1995) a new mathematical model of endwall flows was introduced, eliminating the need for correlations of secondary and tip clearance losses and deviations. The present paper describes how this model, allied to using design-point profile loss and deviation computations and the off-design profile loss and deviation correlation described in the next section, has been set up, and applies it to those test cases.

2. THE CALCULATION METHOD

2.1 The profile loss and deviation correlation

There are many empirical correlations for estimating the profile loss and deviation of cascades. Most of them were derived from experimental measurements on conventional families of aerofoils such as the NACA 65 series, or double circular arc (DCA) aerofoils. The NASA SP36 correlation (Johnsen and Bullock, 1965) is perhaps the best known. The available correlations were reviewed for AGARD by Çetin *et al* (1987), who introduced suggested improvements. More recently, Miller and Wasdell (1987) and Wright and Miller (1991) made another attempt, and so did Kōnig *et al* (1993).

The general approach in almost all these methods has been to identify one or more reference conditions, such as "nominal incidence", to correlate results at that reference condition, and then to estimate the performance at other conditions by "off-design" corrections based on change of incidence or change of diffusion factor from the reference condition. Nowadays, however, aerofoil shapes can be tailored to provide better performance than DCA blades, especially in transonic conditions. No published correlation can predict the

performance of such a cascade, especially in the critical matter of deviation. König, therefore, adopted the idea of applying a simple singularity scheme to the actual blade shape to predict deviation. But this also seems unconvincing for a supersonic aerofoil with separation due to the shock/boundary layer interaction.

The present approach is to adopt a compromise: to compute the "design" performance explicitly from the actual aerofoil shape using a viscous-inviscid interaction method (Calvert, 1982), and then to employ a correlation to estimate the *changes* in deviation and loss from the design condition. Two schemes were tried: the Swan off-design schemes (based on change of diffusion factor) used in SP36, and the Miller scheme (based on change of incidence). The latter proved much more satisfactory in the present context.

Wasdell and Miller (1987) adopted four reference conditions: minimum-loss incidence (i_{ml}), optimum incidence (i_{opt}), stalling incidence (i_s), and choking incidence (i_c). They devised correlations to enable optimum incidence and stalling incidence to be derived from the stagger, camber, and pitch/chord ratio of any DCA cascade. The minimum loss incidence and the choking incidence are functions also of the inlet relative Mach number. Later, Wright and Miller (1991) gave a new simple correlation for minimum-loss incidence. They then adopted "universal" curves relating off-design deviation and loss changes to these four reference incidences.

The present scheme adopts the same four reference conditions plus a fifth, negative-incidence stalling incidence (i_{neg}). The same correlations for minimum-loss incidence, stalling incidence, and optimum incidence are used, but an explicit calculation of the throat area of a DCA cascade is used instead of Miller's correlation. (The throat area appears in the expression for minimum-loss incidence.) Then in place of a 1948 correlation for choking incidence, an explicit calculation is used. The negative-incidence stall figure is needed for a low-speed cascade which does not choke at any incidence, just to provide an alternative reference point at negative incidence.

The "design" condition at which the explicit computations of blade element performance are done is normally the design point of the compressor as a whole. Of course, each individual aerofoil section is not operating at its "optimum incidence" (the point at which the reference value of deviation is correlated by Miller) or at its "minimum-loss incidence" (Miller's reference condition for loss coefficient), though it is unlikely to be far away from them. So the first step in the present method is to evaluate the reference incidence values and then work back from the actual "design" incidence, deviation, and loss coefficient to the deviation at optimum incidence (δ_{opt}), and to the minimum loss coefficient (ω_{ml}). Then at every off-design condition, the local deviation (δ) and loss coefficient (ω) are estimated from δ_{opt} and ω_{ml}.

Figure 1 illustrates the procedure. Fig. 1a shows the off-design deviation correlation, and on it is marked the design

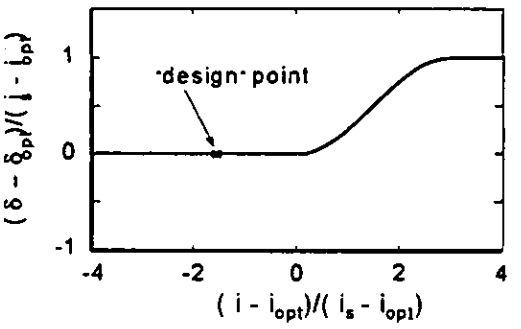

(a) deviation

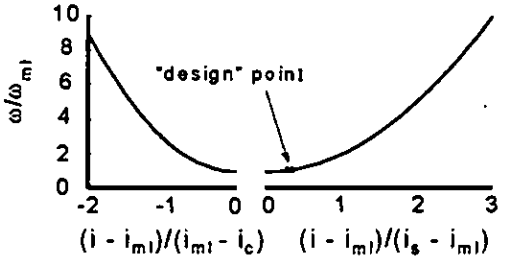

(b) loss coefficient

Figure 1 Miller's off-design correlation

point for a typical rotor blade element of the low speed compressor used later in this paper as a test case. The design incidence is -4.2° and the design deviation is 7.6°. From the curve δ_{opt} is seen to be also 7.6° at the optimum incidence of 1.1° (since the design incidence is less than the optimum incidence). Then Fig. 1b shows the loss coefficient correlation, and on it is marked the design point, at which the loss coefficient is 0.03, from which the minimum loss coefficient of 0.0275 is deduced at the minimum loss incidence of -8.0°. Then from these curves the deviation and loss coefficient of that blade element at any other incidence can be found.

For a cascade with supersonic inlet flow, shock losses must also be added. These losses are estimated using the SP36 method. If the "design" condition at which the explicit computation of losses is made involves some supersonic sections, the SP36 shock loss is subtracted from the computed loss before evaluating ω_{ml}, and then at each off-design condition the appropriate shock loss must be added to the subsonic ω.

The details of all these calculations, except the shock losses (not used in the reported examples) are given in the Appendix.

None of these details apply to the inlet guide vanes, for which no correlation appears to be available; it is assumed that the inlet guide vanes always operate at the same incidence. If the vane stagger changes, new values of outlet gas angle and loss coefficient must be supplied.

2.2 The endwall model

The mathematical model of the endwall flows, secondary flows, and spanwise mixing described by Dunham (1993, 1995), and implemented in a code known as SC92H, does not assume that the compressor is operating at its design point, and in principle it should be applicable off-design. The model calculates the loss and deviation within the annulus wall boundary layers explicitly from the boundary layer velocity profile, and it calculates the secondary loss and secondary deviation outside the boundary layers using secondary flow theory, with provision for spanwise mixing by turbulent diffusion and turbulent convection. But there is one feature of the annulus wall boundary layer (AWBL) calculation which is open to question. The expressions chosen by de Ruyck and Hirsch (1988) for the blade defect forces are functions of the gas angles only, and do not involve the blade metal angles at all. So they imply that the endwall and secondary flow phenomena are unaffected by incidence. Although the expressions they chose yield good estimates of most of the cascade results by Salvage (1974) which cover a range of incidence, those tests do not include variations of incidence alone.

It was therefore decided to review the blade defect force assumptions by a "numerical experiment". Computations were undertaken using a three-dimensional Navier-Stokes code based on that of Dawes (1986), referred to as TRANSCode, on a double-circular-arc cascade at a Mach number around 0.3, to see what effect incidence appeared to have on the endwall effects. The pitchwise-average traverses half an axial chord downstream of the cascade computed by TRANSCode were compared with predictions from SC92H. The cascade selected for these computations was the one tested at higher Mach number by Bario *et al* (1982), with an inlet metal angle of 50.2° and an outlet metal angle of 20.3°.

Three different inlet annulus wall boundary layers were tried for a range of cascades and inlet flow angles: firstly, it was assumed that the AWBL approaching the cascade was very thin, so the secondary flow developed only through the cascade; secondly a collateral inlet AWBL of thickness 10% of the span was tried, and finally a skewed AWBL was imposed. All these calculations led to essentially the same conclusions. Figures 2, 3 and 4 show results with the collateral 10% span boundary layer.

The left hand side of Fig. 2 shows how the outlet axial velocity distribution, the outlet gas angle, and the local pressure loss coefficient change as the incidence is varied *for a given cascade*. The right hand side shows the corresponding predictions by the present author's endwall method SC92H. In running SC92H, the profile deviation and loss values were chosen to match the values predicted by TRANSCode at mid-span. The SC92H results are shown as lines joining the points (21 across the full span) selected for the calculation, and are therefore not smooth curves. Looking first at the loss coefficient, it will be seen that as the incidence increases there is a progressive increase in secondary loss, and the broad pattern of the TRANSCode results is followed by SC92H except at -10° incidence, when TRANSCode displays a larger peak near the wall than does SC92H. Looking next at the gas angles, the familiar pattern of secondary flow is seen, increasing in magnitude as the deflection of the gas through the cascade increases. Generally, TRANSCode and SC92H agree quite well, though at -10° incidence, the wall deflection predicted by SC92H is inaccurate. However, the main difference that can be seen is that at the highest incidence of 9° the TRANSCode secondary flow is much stronger than SC92H predicts. (TRANSCode failed to converge above 9° incidence.) The comparison of the axial velocity profiles shows even more clearly the way the pattern changes at high incidence. Inspection of the details of the TRANSCode results suggests that a corner stall is developing, sweeping the AWBL fluid (with its lower momentum and energy) up the suction surface and leaving a much thinner boundary layer on the wall. SC92H is unable to predict this result, but what it does predict is that the shape factor of the AWBL rises sharply as the incidence increases, to 1.93 at 5° incidence, separating by the time 7° incidence is reached (with a shape factor of 2.11).

Figure 3 shows the effect of incidence *at a given inlet gas angle* of 51°, the incidence being varied by changing the blade metal inlet angle. In this case the extremes of incidence are not shown, and it can be seen that the expressions of de Ruyck and Hirsch (1988) for blade defect forces, which ignore metal angles, are reasonably well justified for these unstalled conditions. Figure 4 illustrates the high inlet angle case of 56°, and even here the outlet traverse is not changed dramatically by incidence.

It is concluded, therefore, that it is a reasonable assumption that the endwall effects depend only on gas angles, at least until the endwall stalls. So the SC92H scheme is just as applicable to off-design calculations as it has previously been shown to be for near-design conditions. Also, it appears that inspection of the AWBL shape factor gives some indication of the approach of endwall stall.

It may be of interest to note that each of these TRANSCode computations took around 8 hours on a DEC-Alpha workstation, whereas each SC92H computation took around ten seconds on a (much slower) DEC VAXstation 4000.

3. APPLICATION TO COMPRESSOR TEST CASES

3.1 Application to a low speed research compressor

The off-design version of SC92H, known as SC95G, was applied to two builds of the compressor tested by Robinson (1991). Both had four identical stages of blading, chosen to be representative of current aero engine stage loading. As shown by Dunham (1993), SC92H models quite well the flow

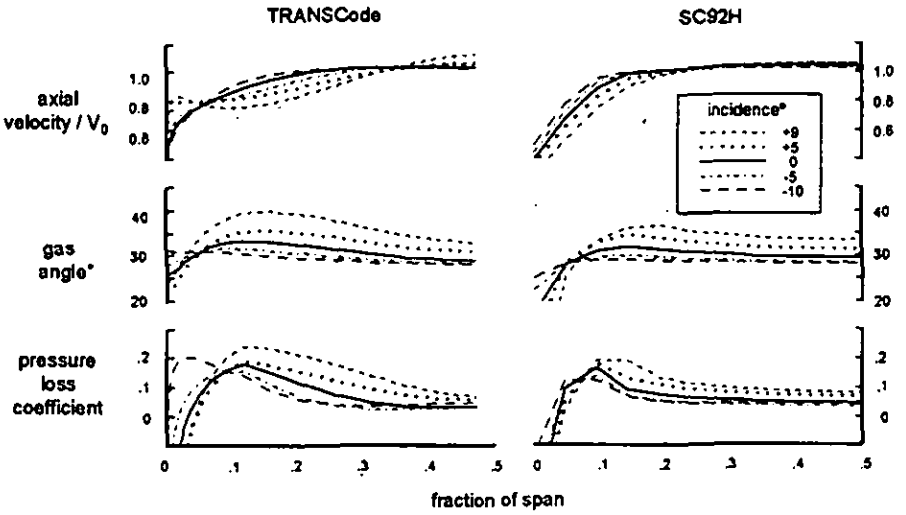

Figure 2 Effect of incidence on a cascade

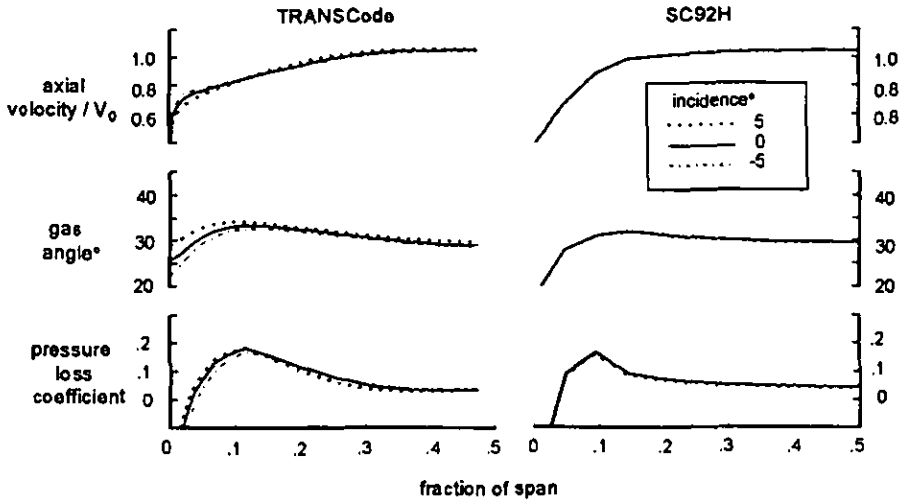

Figure 3 Effect of incidence at constant gas angle

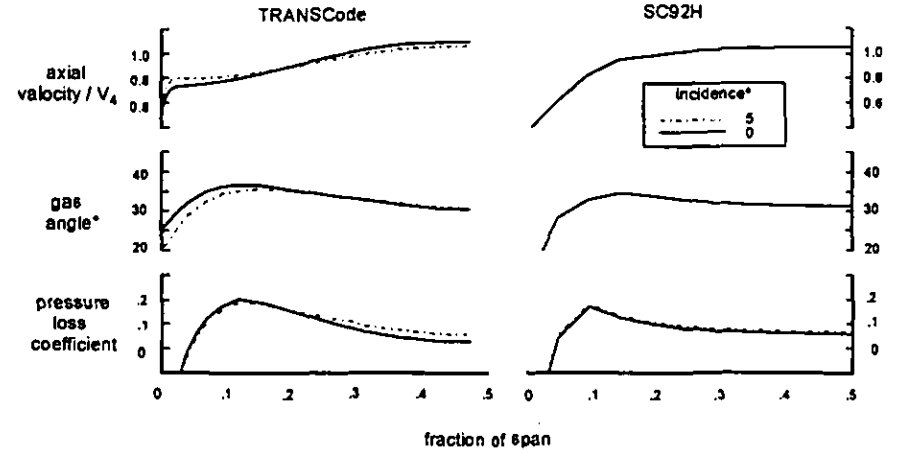

Figure 4 Effect of incidence at constant gas angle, near stall

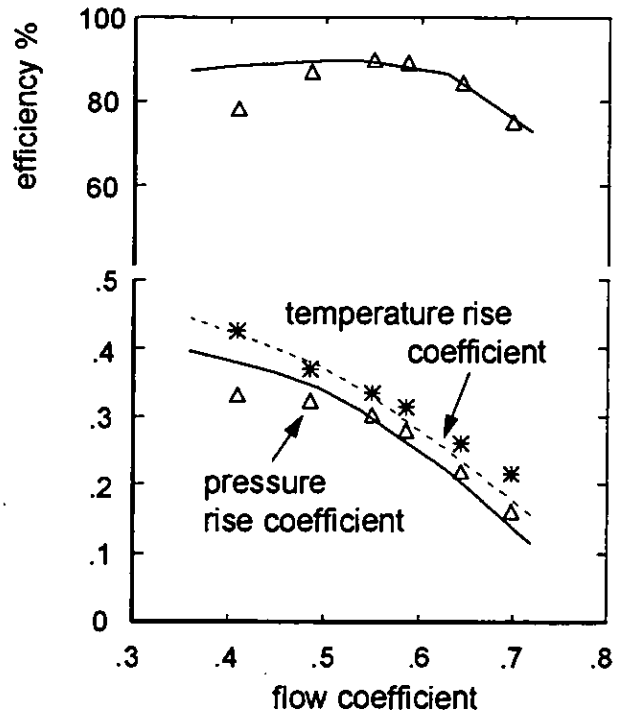

Figure 5 Low speed research compressor: free vortex design

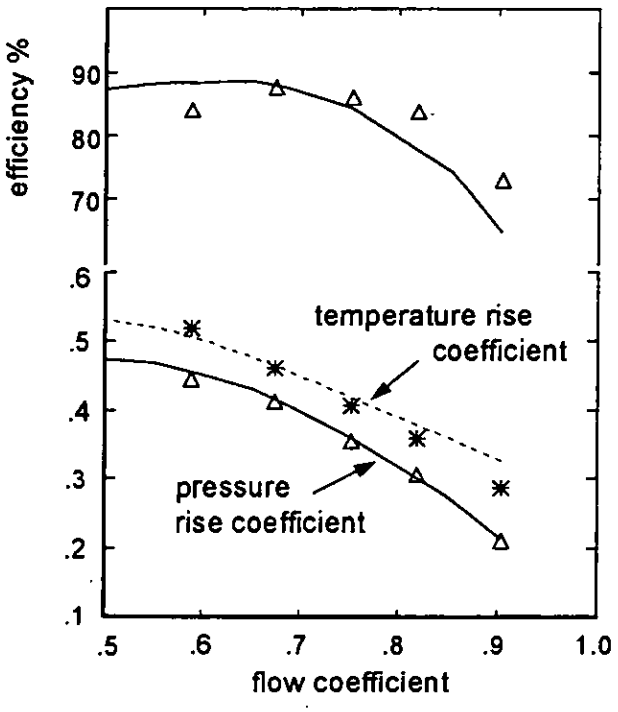

Figure 6 Low speed research compressor: low reaction design

distribution through both builds of this unit at its peak efficiency point. Robinson also measured the full range of compressor performance. In his Thesis, the enthalpy rise was derived from shaft torque measurements, which of course include bearing and windage torque. Subsequently, those effects have been measured (Ahmed *et al*, 1990) and the experimental enthalpy rise and efficiency curves shown here have been corrected accordingly to provide the aerodynamic performance of the blading.

The first build for which predictions were made was the free vortex build, which had DCA blades. Figure 5 shows the average stage performance (i.e. the overall performance divided by 4), in comparison with predictions by SC95G. Many experimental points were measured; for clarity only a small selection of them is shown by the symbols. The predictions are shown by the lines. No blade-to-blade (S1) computations were undertaken for the low speed compressor blading. The profile loss coefficients at the peak efficiency point were assumed to be 0.035 at all radii of both rotors and stators in order to match the observed overall peak efficiency, and the deviations at all radii of all the blade rows at the peak efficiency point were assumed to be 1° lower than Robinson assumed in his design, again in order to match the corrected enthalpy rise at that point.

It will be seen that the off-design temperature rise and pressure rise are underestimated at high flows, showing that the deviation reduces at negative incidence instead of staying constant (as assumed in the Miller correlation). The efficiency is followed quite well over the whole of the characteristic to the right of the peak efficiency point, but as stall is approached SC95G fails to predict the large measured drop in efficiency. (The compressor went into rotating stall at the lowest experimental point shown.) Robinson's analysis of the measured loss distributions at the peak efficiency point and near stall suggests that it is the profile loss that increases far more than SC95G predicts. As the flow is reduced, the AWBL shape factor at the tip of rotor 1 increases, reaching 2.1 (separated) at a flow coefficient of 0.45, though the compressor only stalled at 0.41.

The other build for which predictions were made was the low reaction build, which had modern controlled-diffusion blades. Figure 6 compares predictions with measurements for this case, in the same way. These predictions are less good; it appears that the deviation of these blades increases at high negative incidence, while the corresponding losses increase much less than the correlation *for DCA blades* predicts. At high positive incidence, the efficiency of this blading falls off more than predicted, but less rapidly than for the DCA build. By a flow coefficient of 0.55, the maximum AWBL shape factor has risen only to 1.83; however, the compressor was found experimentally to stall abruptly at a flow coefficient of 0.6.

So the predictions are only fair; but the author is not aware of any better predictions of the overall performance of Robinson's compressors than these.

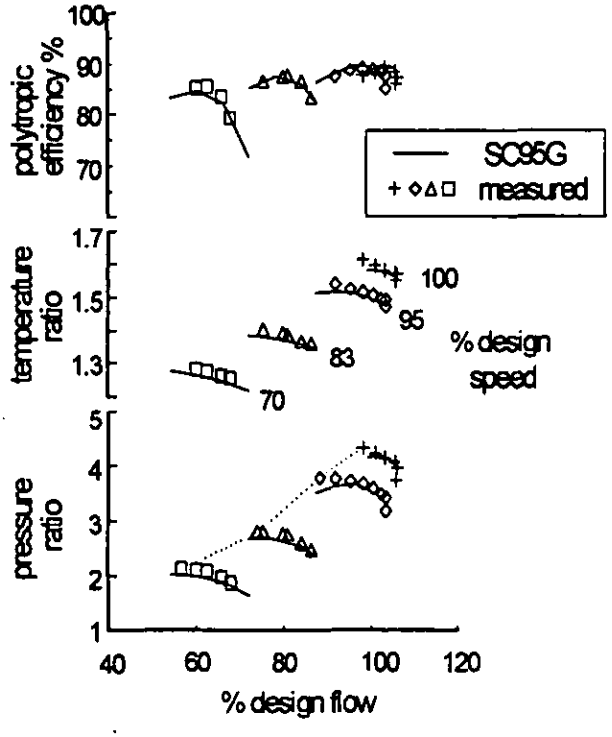

Figure 7 High speed research compressor: build 1

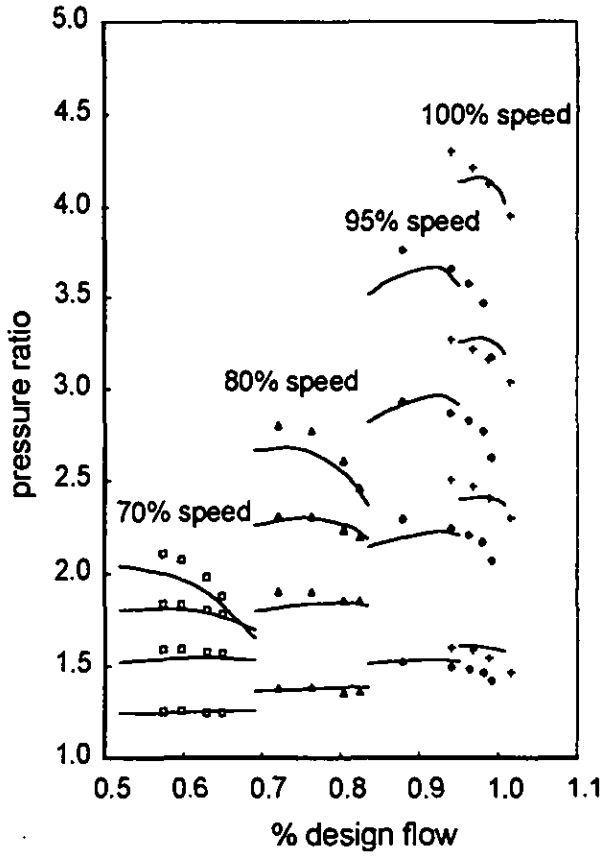

Figure 8 Cumulative stage pressure ratios

3.2 Application to high speed research compressor

The SC95G code was next applied to two different builds of the high speed research compressor C147. This was designed to be representative of an aero-engine core compressor. In making the predictions, the calculated value of stator end clearance and the measured rotor tip clearance were assumed to be constant at the values at which the full traverses were done.

Predictions were first made for the four-stage build 1 (Calvert et al, 1989), which had DCA blading. The points on Fig. 7 show the measured overall performance characteristics, including the surge line (dotted). For the purpose of the SC95G calculation, the "design" point was taken as the peak efficiency point at design speed, at which a full S1-S2 solution had previously been undertaken. This S1-S2 solution gave the results reported in detail in Dunham (1995), and predicted an overall pressure ratio and temperature ratio lower than the measured values. When SC95G was run with the deviation and loss figures produced in this way, it inevitably produced complete characteristics correspondingly below the measured ones. In order to check the off-design operation of the code more directly, the S1-S2 deviation at the "design" point was reduced by 1.5° at all radii on all blade rows except the inlet and outlet guide vanes, which then reproduced the "design" point performance quite well. Figure 7 shows, as lines, the results of the revised SC95G calculations. It will be seen that the temperature ratio variation is followed quite well, although the off-design deviation is slightly high; the efficiency follows the observed pattern well, so the loss predictions must be fair; and therefore the pressure ratio is also reasonably close to measured values. The choking of the compressor, giving rise to vertical characteristics at design speed, is also predicted; solutions cannot be obtained at mass flows slightly above the observed maximum. (At higher mass flows, the code detects the choking and reduces the mass flow.)

At the stalling end of the characteristics, SC95G calculations would run to somewhat lower flows than the observed surge flow (though they might not converge). As the flow was reduced, the AWBL calculations showed increasing values of shape factor, the highest value being invariably at the tip of the first stage rotor. At design speed, the shape factor rises to 2.0 before surge is observed, and at 95% speed to 1.9, but at lower speeds the compressor surges at lower values of maximum shape factor. The question of how surge is initiated is discussed in Section 4.2.

Figure 8 compares the cumulative pressure ratio predicted at stage 1 outlet, stage 2 outlet, stage 3 outlet, and the compressor outlet, (shown as lines) with measurements derived from casing static pressures and continuity (shown as points). It will be seen that the pressure ratio of the first three stages is well predicted, but the pressure ratio of the last stage is underpredicted. This error was discussed by Dunham (1995) and attributed to overestimating the annulus wall boundary layer thicknesses in the later stages.

The other build of C147 for which predictions were made was the five-stage build 2 (Ginder, 1991), which had modern controlled-diffusion blading. In this case, the "design" point at which a full S1-S2 iteration was done was the peak efficiency point at 95% of the actual design speed, because it was at that condition that full traverses were made. Once again, the deviation was adjusted, this time by +1.5° to match the "design point" enthalpy rise. The inlet guide vanes were set at different angles at each speed (unlike build I).

Figure 9 makes the comparisons. It will be seen from the temperature ratio predictions that the off-design deviation is again slightly high. The losses predicted by the S1-S2 scheme appear to be low, so the efficiency over the whole characteristics is uniformly high. As a result, the predicted pressure ratio lines are hardly distinguishable from the measured ones except at top speed.

As stall was approached, the largest value of AWBL shape factor was found at the tip of the first rotor, just as for build 1. The surge line values again reduced with speed, from 2.2 at design speed to 1.9 at 95%, 1.8 at 90%, and to even lower values at lower speeds.

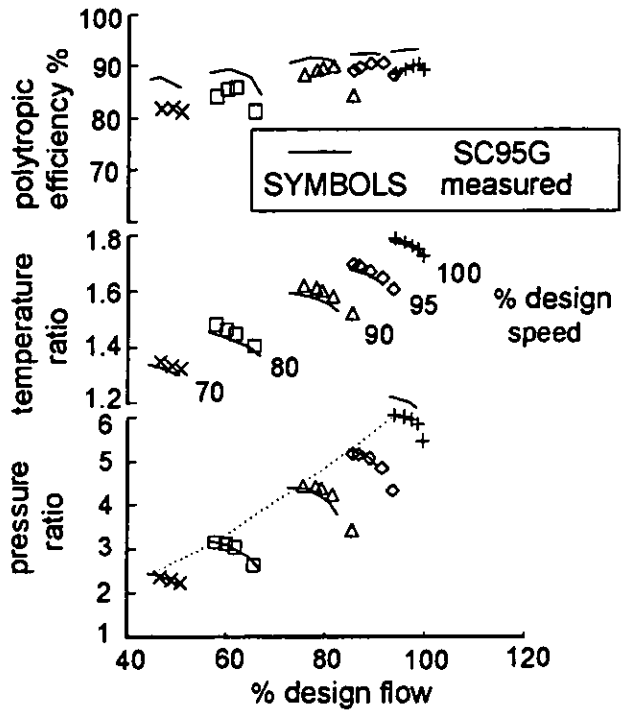

Figure 9 High speed research compressor: build 2

4. DISCUSSION

4.1 Performance prediction

The accuracy of the off-design performance prediction depends on three parameters: deviation, loss, and blockage. The accuracy of the deviation prediction can be judged by looking at the temperature rise predictions, and it does appear to be acceptable for preliminary design studies. The Miller prediction depends very much on the estimate of optimum incidence, and the reason why the SP36 predictions (not shown in this paper) proved to be poor lay in their poor prediction of minimum-loss incidence.

The off-design loss variation can be assessed by looking at the predictions of efficiency change, which were good for the high-speed C147 but not near stall for the low-speed unit. Inspection of the C147 build I predictions shows that the profile losses are generally around twice the secondary losses (defined for this inspection as total loss coefficient minus mean loss coefficient over central half of the annulus) at design speed. Off-design, the secondary loss coefficients do not change greatly, remaining around 0.03, but the profile loss coefficients increase sharply, rising as high as 0.2 at 70% speed. As matching considerations would suggest, the front stages are stalled at low speed, and the back stages encounter negative incidence stall; this happens before they choke. Rotor I stalls just before stator 1, and stator 4 reaches negative incidence stall before rotor 4.

The blockage affects the matching of a high-speed compressor, and in the present method depends on the annulus wall boundary layer predictions. It is not possible to compare the blockage explicitly with measurements, but there is no obvious problem with the C147 results.

The absolute accuracy of the predictions depends critically on the accuracy of the "design point" prediction, as has been made clear by the adjustments found necessary in the examples presented.

4.2 Surge prediction

The question posed in Section 1 was the relationship, if any, between the shape factor H of the annulus wall boundary layer and the observed surge line. It has already been made clear that although peak H values rise sharply as stall (in the low speed unit) or surge (in the high speed unit) is approached, there is no single value of H_{max} at which stall or surge starts. Some relevant parameters are shown in Fig. 10 for Robinson's free vortex build. The lower part of Fig.10 shows how H develops in the first (most critical) stage. The rotor tip is evidently the only place where separation seems

likely, around a flow coefficient ϕ=0.45. However, rotating stall only started at ϕ=0.41. Another possible parameter to identify with stall is the stall margin of individual blade sections, expressed as $(i-i_s)$. On the upper diagram, the mid-height stall margin of the first stage rotor and stator are plotted against flow coefficient ϕ. The stator moves towards stall more rapidly and the stalling incidence is exceeded around ϕ=0.45.

In the case of a high-speed compressor, the situation is greatly complicated by the matching changes over the speed range. At the highest speeds, H_{max} reaches 2.0 at the tip of stage 1 rotor before the mid-height section of the rotor reaches stalling incidence, and the compressor then surges. At lower speeds, stage 1 rotor reaches stalling incidence while H_{max} is well below 1.8, and the compressor surges at a lower flow, but with H_{max} still only about 1.8. The peak values of H_{max} after later blade rows are always lower than those after the first rotor. This is not surprising, as at off-design conditions the first stage is nearest to stall, and has the thinnest incoming boundary layer.

So in none of the examples studied is a visible stall criterion to be found within the SC95G calculations.

4.3 Operating range of blade sections

The preceding Section has shown how the operating range of any individual blade section can be examined using SC95G. Figure 10 shows how the stator of Robinson's free vortex compressor moves faster towards stall than the rotor, for example. The local incidence of the sections of the blading within the annulus wall boundary layers can be examined, though the implications of apparently high local incidence so near the wall seem, from the evidence presented in Section 2.2, to be not as important as might otherwise have been supposed.

5. CONCLUSIONS

The prediction of the complete off-design characteristics of a compressor, except for the surge line, can be accomplished quickly using the method described in this paper. The SC95G code takes of the order of an hour to generate a map like Fig. 7 when each flow is entered manually.

The Miller correlation provided, in the cases examined, an acceptably accurate set of characteristics for both DCA blading and controlled-diffusion blading, at least up to the point at which corner separations apparently became dominant, which SC95G cannot predict.

The shape factor of the annulus wall boundary layer grows sharply as stall or surge is approached, and the location at which that happens seems likely to provide a designer with a strong hint about the region in which his design needs improving; but no correlation has been found between any particular value of shape factor, and stall or surge events.

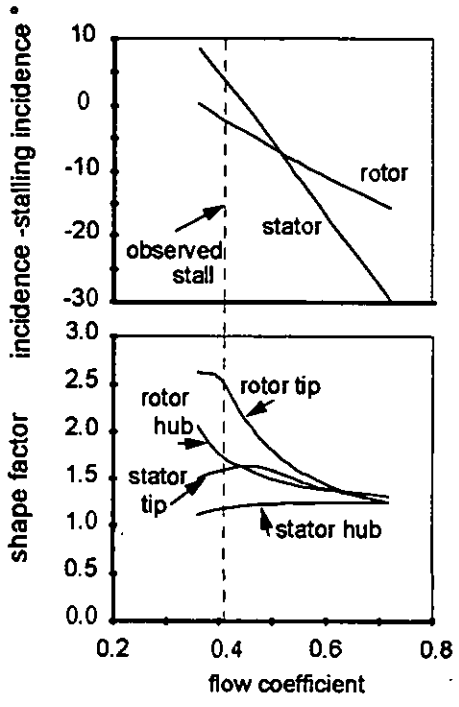

Figure 10 - Stage 1 of the free vortex compressor

It is believed that the use of a two-dimensional method, rather than the earlier one-dimensional methods, will provide the designer with very useful guidance as to the range over which individual blade sections must be designed to operate.

REFERENCES

Ahmed, N.A., Elder, R.L., and McKenzie, A.B., 1990, "Tare Torque Study", unpublished Cranfield Institute of Technology report

Bario, F., Leboeuf, F., and Papailiou, K.D., 1982, "Study of Secondary Flows in Blade Cascades of Turbomachines", *ASME Jnl Engineering for Power*, v.104, p.497

Calvert, W.J., 1982, "An Inviscid-Viscous Interaction Treatment to Predict the Blade-To-Blade Performance of Axial Compressors with Leading Edge Normal Shock Waves", ASME paper no.82-GT-135.

Calvert, W.J. and Ginder, R.B., 1985, "A Quasi-Three-Dimensional Calculation System for the Flow within Transonic Compressor Blade Rows", ASME paper no.85-GT-22

Calvert, W.J., Ginder, R.B., McKenzie, I.R.I. and Way, D.J., 1989, "Performance of a Highly-Loaded HP Compressor", ASME paper no.89-GT-24.

Çetin, M., Üçer, A.S., Hirsch, Ch, and Serovy, G.K., 1987, "Application of Modified Loss and Deviation Correlations to Transonic Axial Flow Compressors", *AGARD Report R-745*

Dawes, W.N., 1986, "A Numerical Analysis of the Three-Dimensional Flow in a Transonic Compressor Rotor and Comparisons with Experiment", ASME paper no. 86-GT-16

de Ruyck, J. and Hirsch, Ch., 1988, "A Radial Mixing Computation Method", ASME paper no.88-GT-68.

Dunham, J., 1993, "A New Approach to Predicting Annulus Wall Boundary Layers in Axial Compressors", *Proc I Mech E, London*, v.207, Pt C, p 413

Dunham, J., 1995, "A New Endwall Model for Axial Compressor Throughflow Calculations", *ASME Jnl of Turbomachinery*, v 117, p 533

Ginder, R.B., 1991, "Design and Performance of Advanced Blading for a High-Speed HP Compressor", ASME paper 91-GT-374

Howell, A.R., Calvert, W.J., 1978, "A New Stage Stacking Technique for Axial-Flow Compressor Performance Prediction", ASME paper 78-GT-139

Johnsen, I.A., Bullock, R.O. (eds), 1965, "*Aerodynamic Design of Axial-Flow Compressors*", NASA SP-36

König, W.M., Hennecke, D.K., Fottner, L., 1994, "Improved Blade Profile Loss and Deviation Angle Models for Advanced Transonic Compressor Bladings", ASME papers 94-GT-335 and 336

Miller, D.C. and Wasdell, D.L., 1987, "Off-Design Prediction of Compressor Blade Losses", *I.Mech.E. Conference Proceedings* CP 1987-6, paper C279/87

Robinson, C.J., 1991, "End-Wall Flows and Blading Design for Axial Flow Compressors", Cranfield Institute of Technology Ph.D.Thesis.

Salvage, W.J., 1974, "Investigation of Secondary Flow Behaviour and End Wall Boundary Layer Development through Compressor Cascades", VKI Report TN-107.

Wright, P.I. and Miller, D.C., 1991, "An Improved Compressor Performance Prediction Model", *I.Mech.E. Conference Proceedings* CP 1991-3, paper C423/028

APPENDIX
THE PROFILE LOSS AND DEVIATION CALCULATIONS

1. Calculation of reference incidence values

Miller and Wasdell gave the following empirical formulae, due originally to Raley:-

stalling incidence $i_s = A + B/(s/c) - C\theta$,

optimum incidence $i_{opt} = X + Y/(s/c) - Z\theta$,

where s/c = pitch/chord ratio

θ = camber°

and the constants were graphical functions of stagger ξ°. The present author found that linear or quadratic expressions fitted their curves well:-

$$A = 7.30 + 0.192\xi - 0.00182\xi^2$$

$$B = 8.01 - 0.1126\xi$$

$$C = 0.1405 + 0.009423\xi - 0.00007339\xi^2$$

$$X = -1.82 + 0.3226\xi - 0.002245\xi^2$$

$$Y = 6.54 - 0.0915\xi$$

$$Z = 0.100 + 0.008434\xi - 0.00004536\xi^2$$

Wright and Miller gave: minimum loss incidence

$$i_{ml} = \cos^{-1}\left[\frac{o/s}{0.155M_1 + 0.935}\right] - \beta_1$$

where o/s = throat/pitch

M_1 = relative inlet Mach number

β_1 = inlet blade metal angle°

Simple continuity yields the following expression for the inlet gas angle α_{1c} at which the throat chokes:

$$\cos\alpha_{1c} = \frac{1}{M_1}\left[\frac{1 + \frac{\gamma-1}{2}M_1^2}{\frac{\gamma+1}{2}}\right]^{\frac{\gamma+1}{2(\gamma-1)}} .(o/s)$$

If the right hand side exceeds unity, as it will at low Mach number, clearly the cascade cannot choke; otherwise

choking incidence = $\alpha_{1c} - \beta_1$.

In order to provide for low Mach numbers, the present author has assumed that the cascade encounters negative incidence stall at the corresponding leading edge incidence to positive incidence stall, namely at

$$i_{neg} = i_{ml} - (i_s - i_{ml}) = 2i_{ml} - i_s .$$

2. Calculation of off-design deviation and loss coefficient

The expressions given by Miller and Wasdell are used at incidences above the optimum. For deviation, the reference value is δ_{opt}, the deviation at optimum incidence. At other incidences, Miller specifies the deviation δ by:

$$\frac{\delta - \delta_{opt}}{i_s - i_{opt}} = 0 \quad \text{if } i \le i_{opt}$$

$$= \sin^2\left[\frac{30(i - i_{opt})}{i_s - i_{opt}}\right] \quad \text{if } 0 < \frac{i - i_{opt}}{i_s - i_{opt}} < 3$$

$$= 1 \quad \text{if } \frac{i - i_{opt}}{i_s - i_{opt}} \ge 3 .$$

For losses, the reference value is ω_{ml}, the loss coefficient at minimum-loss incidence i_{ml}. At incidences above i_{ml}, the loss coefficient ω is given by

$$\frac{\omega}{\omega_{ml}} = 1 + \left(\frac{i - i_{ml}}{i_s - i_{ml}}\right)^2$$

and at incidences below i_{ml}, the loss coefficient ω is given by

$$\frac{\omega}{\omega_{ml}} = 1 + 2\left(\frac{i - i_{ml}}{i_c - i_{ml}}\right)^2 \quad \text{or}$$

$$\frac{\omega}{\omega_{ml}} = 1 + \left(\frac{i - i_{ml}}{i_{neg} - i_{ml}}\right)^2 \quad \text{whichever is larger.}$$

The first of these expresses the increase in losses due to choking (which is usually the larger in a high speed compressor), and the second (introduced by the present author) accounts for the increase in losses at negative incidence (which is important in low speed compressors).

The term 'incidence' throughout this paper refers to the conventional cascade definition, the difference between the gas angle far upstream and the camber angle at the leading edge, in degrees. In a throughflow calculation, the gas angle at the leading edge plane, being a pitchwise mean, is equivalent to the far upstream gas angle in a cascade test.

In order to stabilise the earlier loops of the streamline curvature calculation, the loss coefficient is limited to a maximum value of 0.2. Because any deviations and loss coefficients calculated by the correlation for blade sections within the endwall boundary layers are ignored, this limit is not usually operating by the final iteration, but this is specifically checked by the SC95G code.